HIGH-RESOLUTION SPECTROSCOPY OF SELECTED ABSORPTION LINES TOWARD QUASI-STELLAR OBJECTS. I. LYMAN-ALPHA TOWARD PHL 957[1]

FREDERIC H. CHAFFEE, JR.
Smithsonian Institution, Whipple Observatory

RAY J. WEYMANN
Steward Observatory, University of Arizona

DAVID W. LATHAM
Harvard/Smithsonian Center for Astrophysics

AND

PETER A. STRITTMATTER
Steward Observatory, University of Arizona
Received 1982 June 22; accepted 1982 September 24

ABSTRACT

We have observed 90 Å (6000 km s^{-1}) of the Lyα forest in the spectrum of PHL 957 just shortward of its Lyα emission peak ($z_{em} = 2.69$). At our resolution of 12 km s^{-1} (FWHM), all four absorption features that we detected are fully resolved. We identify all four as Lyα lines arising in intergalactic clouds.

The strongest single absorption line has a Doppler width of 40 km s^{-1}. If this is typical of all strong Lyα lines, the detection of deuterium in these clouds will be very difficult, because the D Lyα line will be swallowed by the Doppler core of Lyα at any column density high enough to produce a strong D Lyα.

The weakest line has a Doppler width of 14.5 ± 2.5 km s^{-1}, which corresponds to an upper limit of 16,700 K for the temperature of the absorbing gas. This is well below the 45,000 K lower limit calculated for the equilibrium temperature of typical metal-free extragalactic clouds. We suggest either that this particular cloud consists of processed rather than primordial material, with the extra cooling provided by metal lines, or that the material is in thin sheets rather than spherical clouds.

Subject headings: galaxies: intergalactic medium — quasars

I. INTRODUCTION

At high resolution, QSO spectra show a dramatic increase in the number of absorption lines shortward of the Lyα emission peak. Lynds (1971) suggested that most of these are Lyα lines arising in material at various intervening redshifts. This interpretation has been strengthened by subsequent studies (e.g., see Young *et al.* 1979; Sargent *et al.* (SYBCW) 1979; and Sargent *et al.* (SYBT) 1980). SYBT observed six QSOs with a spectral resolution of 45 km s^{-1} and argued that the vast majority of the Lyα lines belong to "an intergalactic population which is not associated with galaxies," while only the absorption systems associated with strong Lyα and metal lines arise in the halos of intervening galaxies. The existence of intergalactic clouds would have important implications: (*a*) Such clouds might have survived unscathed from the early stages of the universe and thus might be composed of "primordial," unprocessed material. The detection of deuterium in such a cloud (Adams 1976) would be especially interesting, because it would give a direct determination of the primordial

deuterium abundance. (*b*) The clouds would be heated by the ultraviolet radiation from the general field of QSOs and cooled by collisional ionization and excitation, recombination, and bremsstrahlung. Calculations for typical metal-free clouds indicate that the equilibrium temperatures would be at least 45,000 K (Black 1981). At these temperatures the Doppler width of Lyα should be broad enough to be resolved observationally.

We undertook the present study of a high-redshift QSO with the goal of fully resolving, for the first time, lines in the Lyα forest to set limits on the temperature of intergalactic clouds and to look for suitable candidates for the detection of deuterium.

II. OBSERVATIONS

PHL 957 is one of the few bright ($B = 17.0$) QSOs in the northern hemisphere with sufficiently high redshift ($z_{em} = 2.69$) to place Lyα at a wavelength which could be observed easily with the photon-counting Reticon (Latham 1982), echelle spectrograph (Chaffee 1974), and image stacker (Chaffee and Latham 1982) on the Multiple Mirror Telescope. The Reticon is a one-dimensional detector, and it records only 25 mm of spectrum per exposure, giving roughly 3000 km s^{-1} of

TABLE 1

PHL 957 SPECTRA WITH RESOLUTION BETTER THAN 160 km s^{-1}

Reference	Wavelength Range (Å)	Rc (km s^{-1})
1. Lowrance et al. 1972	4270–4495	52
2. Wingert 1975	3550–4500	46
3. Coleman et al. 1976	3140–5600	150
4. Sargent et al. 1980	3550–5240	45
5. Present work 1982	4427–4465	12
6. Present work 1982	4488–4528	24

coverage independent of the echelle order used. Since PHL 957 is a faint object for such high dispersion (~ 1.8 Å mm^{-1} at $\lambda 4550$), the exposure times were long, and just two wavelength regions were selected for observation.

The published high-resolution observations of PHL 957 are summarized in Table 1, and a portion of the spectrum near the Lyα emission peak at $\lambda 4590$, reproduced from Coleman et al. (1976), is plotted in Figure 1. The regions that we observed are marked A and B on Figure 1. Figure 2 is the sum of twelve 30-min MMT exposures of region A, taken with a 1″25 slit projecting to about 12 km s^{-1} (100 μm) at the detector. The instrumental resolution measured from the sum of all the Th-Ar comparison exposures is 11.5 km s^{-1} (FWHM). This corresponds to about 8 pixels (more than twice the detector resolution), so our spectra are well oversampled. The contribution from the sky was negligible, but the dark rate of about 7 counts per hour per pixel comprised nearly half the total signal. Thirty-minute dark exposures were taken each night, fitted with a second-order polynomial and subtracted from the QSO spectra. Because of this dark correction, the signal-to-noise ratio of the final spectrum shown in Figure 2 is somewhat worse than might be expected from the

Poisson statistics of the net counts. Note that the shape of the continuum in Figure 2 has not been corrected for the instrumental response.

Our exposures of region B, which were taken with a resolution of 24 km s^{-1}, contain only one clearly detected line at $\lambda 4495$, and we do not reproduce them here.

III. LINE IDENTIFICATIONS

The wavelength scale in Figure 2 was generated by fitting a fifth-order polynomial to approximately 20 Th-Ar lines. The rms residuals from this fit suggest that the scale is accurate to about ± 0.01 Å. In this section we discuss the identification of each of the four detected absorption features, the three labeled a, b, and c in Figure 2 and the single line at $\lambda 4495$ in region B.

a) $\lambda 4438$

We identify the line at $\lambda 4437.8$ as a Lyα line because its corresponding Lyβ can be seen weakly in Coleman et al.'s (1976) spectrum at $\lambda 3744.6$, within 0.2 Å of its predicted position. Wingert (1975) also suggests that $\lambda 4438$ is Lyα, based on his detection of the corresponding Lyβ.

b) $\lambda 4442$

The line whose identity is the most difficult to establish is the narrow unsaturated feature at $\lambda 4442.4$. Its equivalent width is ~ 14.5 km s^{-1} (~ 215 mÅ: we express line strengths as well as spectral resolutions in velocity units because such units are independent of redshift, i.e., $W_v = W_\lambda c/\lambda$). If this line were Lyα ($z = 2.654$), its Lyβ would lie at $\lambda 3748.3$ and would have a strength of 2.7 km s^{-1} (~ 40 mÅ), much too weak to be detected in any of the spectra listed in Table 1. Because our detector is not sensitive below $\lambda 3900$, we were unable to search for this Lyβ.
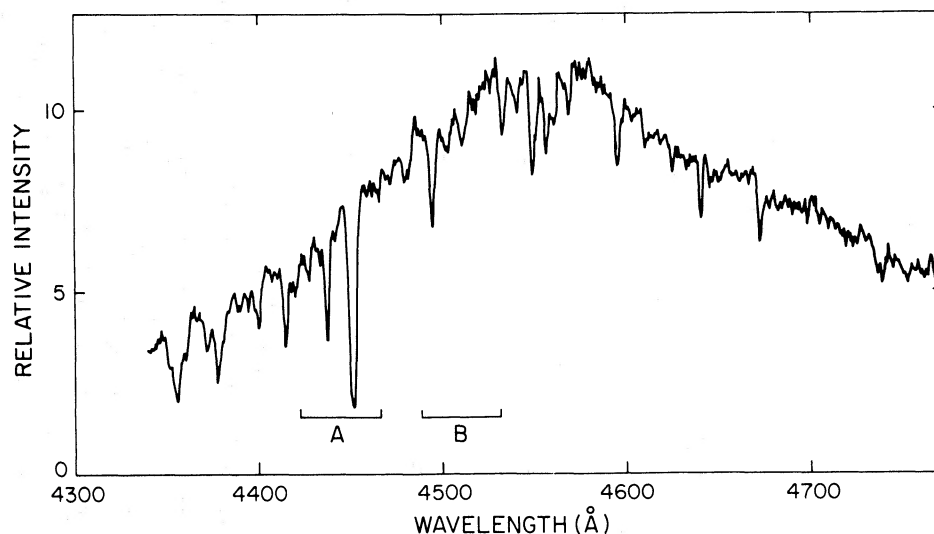

FIG. 1.—A portion of Coleman et al.'s (1976) 150 km s^{-1} resolution spectrum of PHL 957. The present work presents data on regions A and B observed at resolutions of 12 and 24 km s^{-1}, respectively.
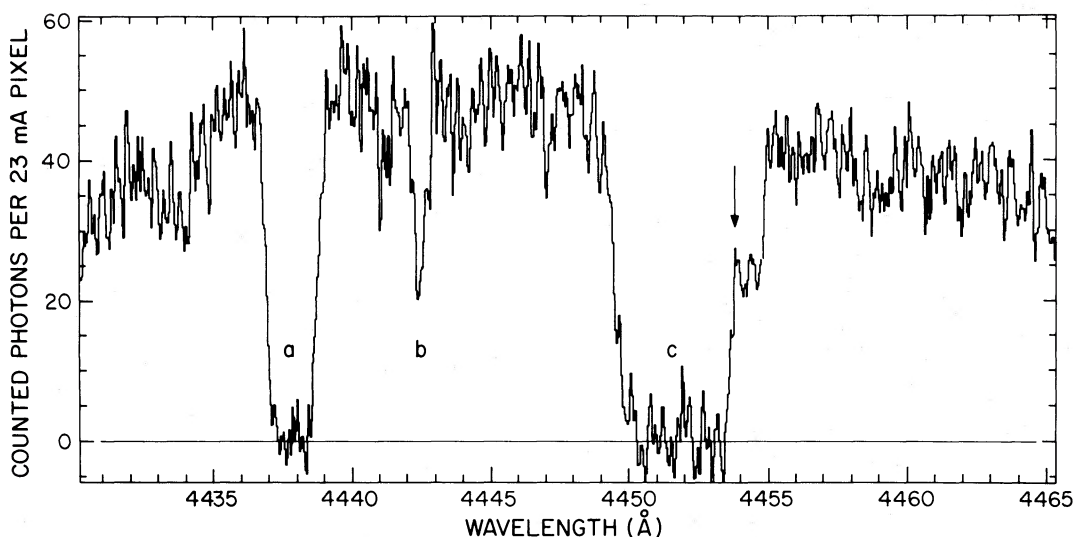
Fig. 2.—MMT echelle spectrum of region A in Fig. 1 at 12 km s^{-1} resolution. Lines marked a, b, and c are discussed in §§ IIIa, b, and c, respectively. The arrow marks where Mg II $\lambda2803.5$ should lie if feature b were Mg II $\lambda2796.3$.

Another way to confirm that $\lambda4442$ is a Lyα line is to reject all other plausible candidates. We used our data to eliminate close doublets with separations less than about 1000 km s^{-1}. Many other metal lines were eliminated by searching Coleman et al.'s data for the corresponding Lyα and metal lines with the same redshift. In column (1) of Table 2 we list the candidates that we considered, column (2) gives their rest vacuum wavelength, and column (3) gives the reason for rejection. The entry CWLS in column (3) indicates that the rejection was based on our data. Of all the plausible candidates, only Mg II $\lambda2796.3$ could not be rejected easily. In this case Mg II $\lambda2803.5$ would lie in the wing of $\lambda4452$ at the location marked by the arrow in Figure 2. It appears that the structure in the wing of $\lambda4452$ is not at the proper wavelength nor of the proper strength to be Mg II $\lambda2803.5$. We thus conclude that $\lambda4442.4$ is very likely a weak Lyα line with $z = 2.655$.

c) $\lambda4452$

The extreme breadth of $\lambda4452$ (~ 135 km s^{-1} FWHM) led Wingert (1975) to suggest that this feature is a close Lyα pair. This interpretation is confirmed by the apparent splitting of $\lambda3756$ on his spectrum at the position of the corresponding Lyβ.

d) $\lambda4495$

The identification of the single feature in region B as a Lyα line is unconfirmed. Its Lyβ would be too weak to be detected on any of those listed in Table 1. Our observations show that, as with $\lambda4438$ and $\lambda4452$, its core is opaque. Thus the cloud in which it arises must cover the QSO emission-line region. This allows us to estimate a lower limit for the size of the cloud, which will be important when we consider the physical conditions of such clouds in § V.

IV. $\lambda4438$ AND THE D/H RATIO

The Lyα line at $\lambda4438$ has an equivalent width of 125 km s^{-1}, and from spectra 2 and 3 in Table 1 we estimate the strength of the corresponding Lyβ ($\lambda3744$) to be 36^{+20}_{-10} km s^{-1}. Application of a curve of growth

TABLE 2
REJECTED CANDIDATES FOR THE IDENTITY OF $\lambda4442$

| Ion (1)	λ_{vac} (2)	Reason for Rejection (3)
C II	1334.5	Lyα at $\lambda4046.8$
C III	977.0	Lyα at $\lambda5527.6$
C IV	1548.2	Lyα at $\lambda3488.2$
C IV	1550.8	C IV ($\lambda1548.2$) at $\lambda4435.0$ (CWLS)
N V	1242.8	N V ($\lambda1238.8$) at $\lambda4428.1$ (CWLS)
N V	1238.8	N V ($\lambda1242.8$) at $\lambda4456.7$ (CWLS)
O I	1302.2	Lyα at $\lambda4147.2$
O VI	1031.9	Lyα at $\lambda5233.5$
O VI	1037.6	Lyα at $\lambda5204.8$
Mg II	2803.5	Mg II ($\lambda2796.5$) at $\lambda4431.0$ (CWLS)
Al II	1670.8	Al III ($\lambda1862.8$) at $\lambda4952.9$
Al III	1862.8	C IV at $\lambda\lambda3692.1, 3698.3$
Al III	1854.7	Al III ($\lambda1862.8$) at $\lambda4461.8$ (CWLS)
Si II	1190.4	Lyα at $\lambda4536.7$
Si II	1193.3	Si II ($\lambda1190.4$) at $\lambda4431.6$ (CWLS)
Si II	1260.4	Lyα at $\lambda4284.7$
Si II	1304.4	Si II ($\lambda1260.4$) at $\lambda4292.6$
Si II	1526.7	Lyα at $\lambda3537.4$
Si III	1206.5	Lyα at $\lambda4476.2$
Si IV	1393.8	Lyα at $\lambda3874.7$
Si IV	1402.8	Lyα at $\lambda3849.8$
Fe II	1144.9	Lyα at $\lambda4717.0$
Fe II	1608.5	Lyα at $\lambda3357.5$
Fe II	2382.0	Mg II at $\lambda\lambda5215.1, 5228.5$
Fe II	2585.9	Fe II ($\lambda2599.4$) at $\lambda4465.6$
Fe II	2599.4	Mg II at $\lambda\lambda4778.9, 4791.2$
Fe II	2366.9	Fe II ($\lambda2373.7$) at $\lambda4455.2$ (CWLS)
Fe II	2373.7	Fe II ($\lambda2382.0$) at $\lambda4457.9$ (CWLS)
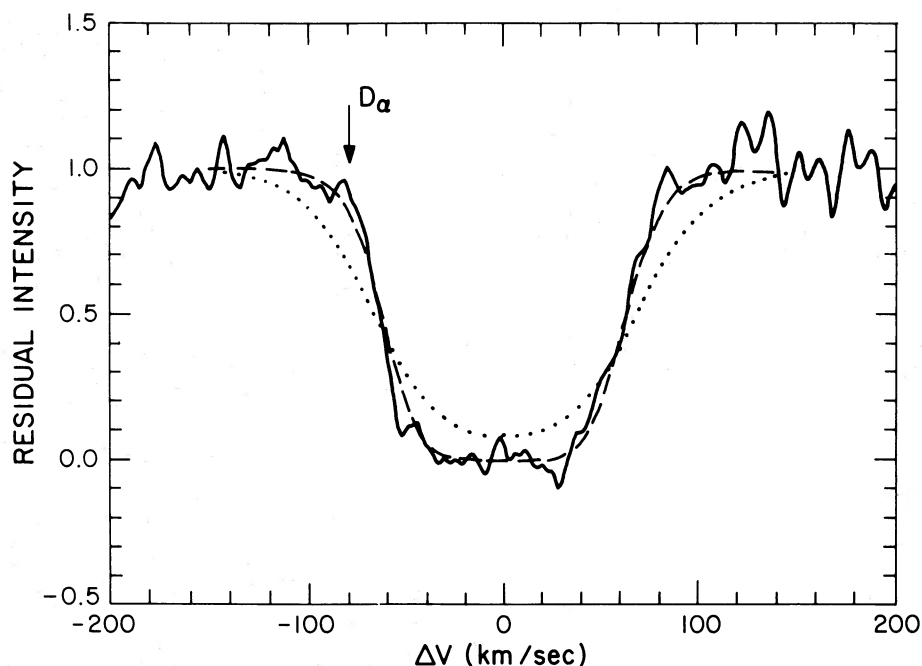
Fig. 3.—(a) Voigt profile fit to the λ4438 line data. The dotted curve is the theoretical Lyα profile for $N(H^0) = 2.0 \times 10^{14}$ cm^{-2} and $b = 60$ km s^{-1}—the parameters which result from a curve of growth analysis of the Lyα and Lyβ equivalent widths. The dashed curve is the best fit by eye still allowed by the curve of growth analysis—namely, $N(H^0) = 4.4 \times 10^{14}$ cm^{-2} and $b = 40$ km s^{-1}. This better fit to the profile is used for our analysis. The arrow marks the expected location of the D Lyα line.

to these line strengths yields log $N(H^0) = 14.32^{+0.25}_{-0.29}$ cm^{-2} and $b = 60^{+\infty}_{-20}$ km s^{-1}, where $N(H^0)$ is the column density of neutral hydrogen atoms and b is the Doppler width. Since we have clearly resolved this line, we can also fit theoretical profiles in order to derive values of $N(H^0)$ and b. Morton and Morton (1972) used this technique and found log $N(H^0) = 14.32^{+0.35}_{-0.15}$ cm^{-2} and $b = 40 \pm 10$ km s^{-1} for their observations of λ4438. In Figure 3 we show two Voigt profiles which have been convolved with our instrumental profile and plotted on the observed λ4438 line. The dotted profile was calculated for the $N(H^0)$ and b derived from the curve of growth, while the dashed profile is the best fit that is still allowed by the limits set by the curve of growth. The latter profile better matches the λ4438 feature, and we adopt its parameters, namely,

$$\log N(H^0) = 14.64 \text{ cm}^{-2}, \quad b = 40 \text{ km s}^{-1}.$$

The isotopic shift for D Lyα is -81 km s^{-1}, and its expected location is marked in Figure 3. Even a 1 σ upper limit of 5 km s^{-1} for its equivalent width implies D/H $< 10^{-2}$, a limit of little significance since values between 10^{-4} and 10^{-5} are usually found in the Galaxy. The deuterium question is of sufficient interest that some further remarks regarding its possible detection are justified. Adams (1976) showed that for small Doppler widths (6–10 km s^{-1}) a neutral hydrogen column density in excess of 10^{18} cm^{-2} is required to produce a detectable D Lyα. However, if $b = 40$ km s^{-1} is typical, D Lyα will not be easy to detect in a cloud with such a high column density because the Doppler core of Lyα will

swallow D Lyα. Other recent studies have encountered similar difficulties in searching for deuterium. A search for D Lyα in 0420−388 (Atwood, Baldwin, and Carswell 1982) has yielded no suitable candidates, and Oke and Korycansky (1982) have concluded that b is typically 35 km s^{-1}. Our upper limit of 17 km s^{-1} for the λ4442 cloud indicates that there may be a distribution of Doppler widths for the Lyman lines. This distribution is worthy of further study, since it may dictate whether deuterium can be detected in primordial clouds and in any case will provide important information about the physical characteristics of these clouds.

V. λ4442 AND THE TEMPERATURE OF AN OPTICALLY THIN CLOUD

The narrowest line that we detected, the feature at λ4442, is well resolved by our data. The dashed curve in Figure 4 is a Voigt profile chosen to fit just the shortward wing and core of our observed feature (the case where the structure in the longward wing is assumed to be some other real line), while the dotted curve was chosen to fit the whole λ4442 feature (the case where the red structure is assumed to be noise). Taking these two fitted profiles as the extremes, we infer

$$N(H^0) = (1.8 \pm 0.25) \times 10^{13} \text{ cm}^{-2},$$

$$b = 14.5 \pm 2.5 \text{ km s}^{-1}.$$

The Doppler width allows us to estimate an upper limit for the temperature of the gas: $T \leq Mb/2k$. This gives
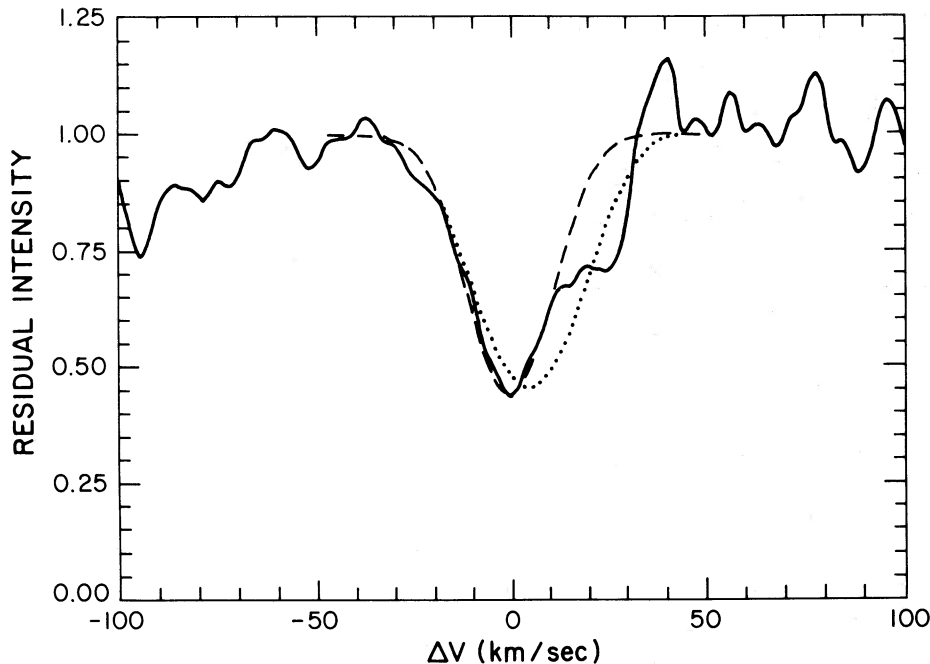
$$T \leq 12,700 \pm 4000 \text{ K}.$$

Fig. 4.—(a) Voigt profile fit to the $\lambda4442$ line data. The dashed curve is the Lyα profile which gives the best fit of the core and shortward wing of the line. Such a fit would be appropriate if the structure on the red wing were another weak line and gives $N(H^0) = 1.6 \times 10^{13}$ cm^{-2} and $b = 12$ km s^{-1}. The dotted curve is the best fit to the overall profile. Such a fit would be appropriate if the structure on the red wing were noise and gives $N(H^0) = 2.1 \times 10^{13}$ cm^{-2} and $b = 17$ km s^{-1}.

When we undertook this study, no careful calculations of the temperature for metal-free intergalactic clouds had been published, although SYBT had suggested that a temperature of the order of 30,000 K was appropriate. To see if a temperature as low as 16,700 K might be possible, we carried out calculations of the ionization and thermal equilibria for clouds of pure hydrogen, ionized and heated by a power-law radiation field from QSOs with a spectral index of 3/4 and a specific intensity of radiation in the Lyman limit of 7.8×10^{-22} ergs s^{-1} cm^{-2} Hz^{-1} sr^{-1}, and cooled by free-free radiation, recombination, and collisional ionization and excitation. The results of our calculations are summarized in Figure 5, where we have plotted the equilibrium relations for log n_t versus T_4 and for log n_t versus log $n(H^0)$. $T_4 = T/10^4$ is the equilibrium temperature, and $n_t = n(H^0) + n(H^+)$ is the total number density of hydrogen.

We can set a limit on the equilibrium temperature if we can pin down the number density of neutral hydrogen in the cloud. This is possible if we assume, as suggested by SYBCW, that in general the intergalactic clouds are bigger in size than the QSO emitting regions. This suggestion is supported by our observation of the $\lambda4495$ feature in PHL 957. It has the redshift closest to that of the QSO itself, yet the core of the feature is opaque. If we adopt 10^{19} cm as a typical diameter for the region emitting Lyα in PHL 957, then the size of our $\lambda4442$ cloud must be larger than this. For a spherical cloud (i.e., not highly flattened) of diameter d, $N(H^0) = dn(H^0)$. For our $\lambda4442$ cloud this gives an upper limit to the density of log $n(H^0) < -6.0$ and a corresponding

lower limit on the equilibrium temperature of $T > 25,000$ K, a value well above the upper limit allowed by our measurement of the width of $\lambda4442$. Furthermore, this conclusion is relatively insensitive to the value adopted for the intensity of the QSO radiation field at the Lyman limit. A higher intensity increases the discrepancy, while an intensity 100 times lower than we assumed decreases the equilibrium temperature that we derive to 17,300 K. Recent calculations by Wolfe (1982) and Weymann et al. (1982) suggest that the actual intensity is at least an order of magnitude higher than we adopted.

We have also considered the possibility that the assumption of ionization equilibrium may not be valid for these low-density clouds, since the recombination time is comparable to or even longer than the time between QSO turn-on (at $z > 3.7$) and the epoch of our observations ($z \sim 2.5$). It can be shown that the time to approach ionization equilibrium is short compared to the recombination time (and also that the cooling time for recombination and thermal bremsstrahlung is comparable to the recombination time at temperatures on the order of 25,000 K). Thus our estimates of the temperatures in metal-free clouds are insensitive to the assumption of ionization equilibrium.

Black (1981) has calculated more detailed models for primordial intergalactic clouds, including the effect of helium and a density gradient obeying hydrostatic equilibrium. He gives convenient relations between n_t, T, and $N(H^0)$ in steady-state clouds. For the clouds with column densities as low as we observe in our $\lambda4442$ cloud, he concludes that the equilibrium temperature is on the
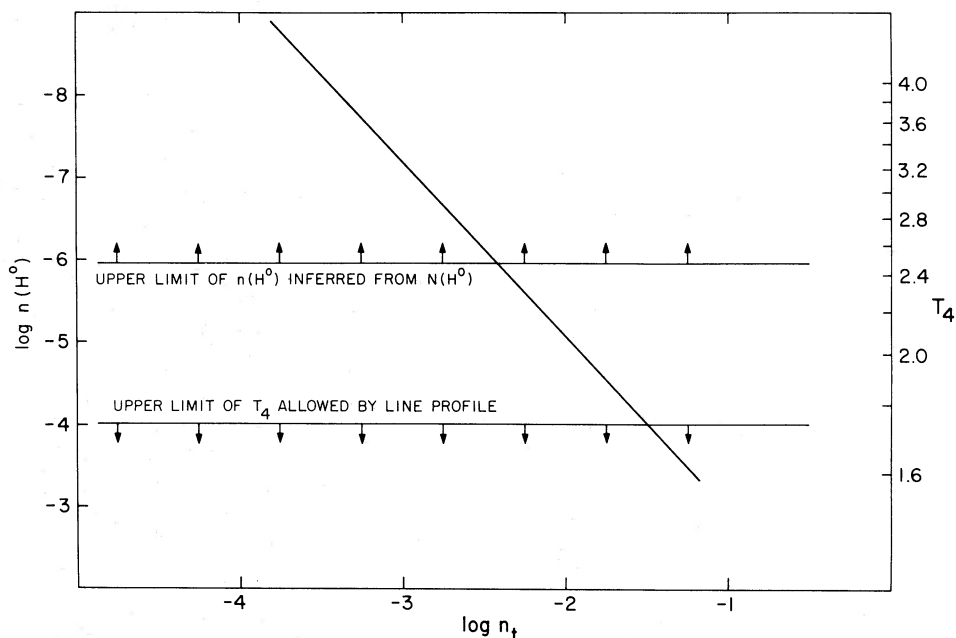
FIG. 5.—The n_t-$n(H^0)$ and n_t-T_4 relations which result from models of pure hydrogen clouds in ionization and thermal equilibrium. The lower limit on $n(H^0)$ is inferred from the observed $N(H^0)$ value and an estimate for the minimum cloud size. The upper limit on T_4 follows from the width of the observed λ4442 profile. No solutions can be found which satisfy both limits.

order of 50,000 K.

Two possible ways for producing the low observed kinetic temperature in the λ4442 cloud are:

1. The cloud is not metal free, and the required cooling is provided by collisional excitation of metal lines. However, recent computations by Ferland (1982) using the radiation field calculated by Weymann et al. (1982) suggest that even with solar metal abundances a cloud having $n(H^0) \lesssim 10^{-6}$ can not cool to 12,000 K.

2. The clouds are not remotely spherical, but are in sheets (Black 1982), thus allowing higher number densities and more cooling for the same observed column density. Black (1982) has estimated that a sheet with a thickness of about 10^{15} cm (i.e., an aspect ratio of at

least 10^4) could be as cool as 12,000 K. Whether such thin sheets can be produced (e.g., by shocks) without additional heating is a problem to be investigated.

REFERENCES

Adams, Thomas F. 1976, Astr. Ap., 50, 461.
Atwood, B., Baldwin, J. A., and Carswell, R. F. 1982, Ap. J., 257, 559.
Black, John H. 1981, M.N.R.A.S., 197, 553.
———. 1982, private communication.
Chaffee, Frederic H., Jr. 1974, Ap. J., 189, 427.
Chaffee, Frederic H., Jr., and Latham, David W. 1982, Pub. A.S.P., 94, 386.
Coleman, G., Carswell, R. F., Strittmatter, P. A., Williams, R. E., Baldwin, J., Robinson, L. B., Wampler, E. J. 1976, Ap. J., 207, 1.
Ferland, G. 1982, private communication.
Latham, David W. 1982, in IAU Colloquium 67, Instrumentation for Large Telescopes, ed. C. M. Humphries (Dordrecht: Reidel), p. 259.
Lowrance, John L., Morton, Donald C., Zucchino, Raul, Oke, J. B., and Schmidt, Maarten. 1972, Ap. J., 171, 233.
Lynds, C. R. 1971, Ap. J. (Letters), 164, L73.
Morton, D. C., and Morton, W. A. 1972, Ap. J., 174, 237.
Oke, J. G., and Korycansky, D. C. 1982, Ap. J., 255, 11.
Sargent, Wallace L. W., Young, P. J., Boksenberg, A., Carswell, R. F., and Whelan, J. A. J. 1979, Ap. J., 230, 49 (SYBCW).
Sargent, Wallace L. W., Young, P. J., Boksenberg, A., and Tytler, David. 1980, Ap. J. Suppl., 42, 41 (SYBT).
Weymann, R. J., Bechtold, J., Green, R., Schmidt, M., and Wolfe, A. 1982, in preparation.
Wingert, David W. 1975, Ap. J., 198, 267.
Wolfe, A. 1982, private communication.
Young, P. J., Sargent, W. L. W., Boksenberg, A., Carswell, R. F., and Whelan, J. A. J. 1979, Ap. J., 229, 891.

FREDERIC H. CHAFFEE, JR.: Smithsonian Institution, P.O. Box 97, Amado, AZ   85640

DAVID W. LATHAM: Center for Astrophysics, 60 Garden Street, Cambridge, MA   02138

PETER A. STRITTMATTER and RAY J. WEYMANN: Steward Observatory, University of Arizona, Tucson, AZ   85721